N90-10803

ADVANCES IN PHOTOGRAPHIC X-RAY IMAGING FOR SOLAR ASTRONOMY

D. Moses and R. Schueller
American Science and Engineering, Inc.
Cambridge, Massachusetts 02139

K. Waljeski
Brandeis University
Waltham, Massachusetts 02254

and

J.M. Davis
NASA, Marshall Space Flight Center
Huntsville, Alabama 35812

ABSTRACT

The technique of obtaining quantitative data from high resolution soft X-ray photographic images produced by grazing incidence optics was successfully developed to a high degree during the AS&E Solar Research Sounding Rocket Program and the S-054 X-Ray Spectrographic Telescope Experiment Program on Skylab. Continued use of soft X-ray photographic imaging in sounding rocket flights of the AS&E High Resolution Solar Soft X-Ray Imaging Payload has provided opportunities to further develop these techniques. The developments discussed include: (1) The calibration and use of an inexpensive, commercially available microprocessor controlled drum type film processor for photometric film development. (2) The use of Kodak Technical Pan 2415 film and Kodak SO-253 High Speed Holographic film for improved resolution. (3) The application of a technique described by Cook, Ewing, and Sutton[1] for determining the film characteristics curves from density histograms of the flight film. Although the superior sensitivity, noise level, and linearity of microchannel plate and CCD detectors attracts the development efforts of many groups working in soft X-ray imaging, the high spatial resolution and dynamic range as well as the reliability and ease of application of photographic media assures the continued use of these techniques in solar X-ray astronomy observations.

1. INTRODUCTION

Photographic detection of X-rays has been an essential technique in the history of X-ray applications since the discovery of the phenomena. X-ray photography has been primarily used as a position sensing (imaging) technique with only qualitative information on dosimetry. However, when sufficient effort is devoted to calibration (in all its various aspects), quantitative measurements of total energy deposit on a photographic medium have been successfully made for many applications.

One particularly successful use of quantitative measurements from photographic X-ray images was developed for the AS&E Solar Research Sounding Rocket Program and the S-054 X-Ray Spectrographic Telescope Experiment Program on Skylab. The details of this approach have been described in a series of papers and presentations[2-5]. In these programs, images of the solar soft X-ray (3-60 Angstroms) corona were formed by grazing incidence optics with angular resolution ranging from 2-5 arc seconds. Since the plate scales for these telescopes range from 7 to 10 microns

per arc second, the plate scale of the detector must be of the order of 7 to 20 microns. Furthermore, it is quite common to observe coronal structures which vary by over three orders of magnitude in soft X-ray emission within a single image; flares can generate a dynamic range of 10^6. At the time of the design of these instruments, photographic film was the only detector suitable for space flight that possessed the required combination of sensitivity, spatial resolution, and dynamic range. Even today, this combination of performance, when coupled with the refinements in technique which are described in this paper, makes photographic media a very attractive choice for quantitative soft X-ray imaging of the solar corona.

2. PHOTOMETRIC DEVELOPMENT PROCEDURE

A large immersion-type continuous flow film processor was designed and built for the Skylab S-054 film processing. This machine was capable of maintaining variations in a test sensitometric visible light exposure to within $\pm$ 0.03 diffuse density units throughout the D log E curve for the film type used in this investigation (Kodak SO-212). Furthermore, the gamma of the test D log E curve was held to 1.50 $\pm$ 0.06. While this machine provided excellent results with the 1300-foot rolls of 70 mm Skylab film, it is poorly suited to the 25-foot rolls of 35 mm film from the sounding rocket investigations because of the differences in the width of film, the difficulties in splicing a sufficient length of leader for the large processor, and the degradation in the machine following long periods of disuse.

Two aspects of the SO-212 film used in both the Skylab and Sounding Rocket investigations complicate the search for alternative solutions to the problem of photometric film processing: (1) The film was manufactured with a 2.5 mil base instead of he standard 4 mil base to reduce the bulk of the film rolls, and (2) the film was manufactured without the usual 1 micron gelatin topcoat to minimize absorption of low energy X-rays. The thin film base makes for serious handling difficulty in a processing system, particularly in loading reels for hand development. The lack of a topcoat makes the film very sensitive to pressure-induced developable artifacts in the handling process. Furthermore, the lack of a topcoat makes the development of the film extremely sensitive to the local concentration of developer chemistry. This difficulty made it impossible to obtain uniform development across the film with any type of hand development attempted by these investigators.

Through the suggestion of R. Haggerty of Crimson Camera Company, Cambridge, Massachusetts, the film processing needs of the sounding rocket program were met by the use of a mass produced, microprocessor controlled film processor manufactured by King Concept Corporation of Minneapolis, Minnesota. The processor is designed around a horizontally positioned light-tight drum into which the reel mounted film is placed. Under microprocessor control, chemistry is introduced and evacuated on a one-shot basis, and agitation is obtained through rotation of the drum. The temperature of the chemistry is maintained within 0.2 degrees centigrade by a water jacket, and the air temperature is controlled in the chamber where the drum is mounted. Kodak HC110 developer was used because of the ease of adjusting and repeatably obtaining the desired dilution. The greatest difficulty in the entire procedure was loading the 25-foot lengths of thin base SO-212 film on the stainless steel reels. This was finally accomplished with a modification to the King Concept Corporation device for film loading and a very practiced hand. Particular care was also devoted to monitor the temperature soak of the process, to avoid contamination effects, and to properly mix and store solutions.

The performance of the processor was monitored through the use of the same visible light sensitometric exposures (step-wedge with density increments of 1.414) as used in the Skylab effort. Visible light exposures were chosen over X-ray exposures based on the issues of ease and repeatability of exposure. The calibration effort consisted of 38 test batches conducted over a three-month interval.

The gamma of the D log E curve was found to vary along the length of the film within a given batch by no more than 0.03 from the mean. The film development batch exhibiting the greatest variation from the target gamma of 1.50 had a gamma of 1.37 (a variation of 0.13), although typical variations from the target value were of the order of 0.05. The extreme variation was obtained during a run significantly separated in time from the previous batches, indicating the need for a calibration run immediately before any flight run to test for changes in chemistry strength, temperature drifts, etc.

Measurement of variations in density throughout the sensitometric step wedges was complicated by the combination of the density structure of the step wedge, the extreme sensitivity of SO-212 film to local chemistry variations, and the direction of flow of the chemistry during agitation. Since agitation was accomplished in the drum by continuous rotation, the chemistry flow was constant and unidirectional along the length of the film. The length of the sensitometric step wedge was such that it could only be oriented with step exposures either increasing or decreasing along the length of the film. Therefore, the "downstream" density steps were always exposed to developer which was partially exhausted by the upstream density steps. While this developer exhaustion effect was never detected between two successive step wedges, the effect was always apparent within an individual step wedge. If the orientation of the sensitometric exposure was such that the more heavily exposed steps were "upstream" in the flow of the developer, the densest steps would have higher values and the less dense steps would have lower values than the case in which the least exposed steps were oriented "upstream." The two D log E curves would cross in the transition between the shoulder and straight line region with the greatest differences being restricted to the shoulder region (thus minimizing differences in gamma).

The variables of developer dilution, temperature, rotational agitation speed, rotational agitation direction (cw vs. ccw), and development time were explored and adjusted -- within the constraint of the target gamma value of 1.5 -- to minimize the effects of the developer depletion along flow direction. The resulting optimal development parameters were found to be dilution D of HC110 at 20°C for 3.75 minutes with 60 RPM rotational speed and a flow direction opposite that of the standard process. Within a single roll of film, density variations of 0.03 were found between step wedges of similar orientation with respect to developer flow direction. For step wedges of opposite orientation, the straight line portions were found to differ by less than 0.06 density units within a given roll of film while individual steps in the shoulder region could differ by as much as 0.12 density units. The density variations from roll to roll are in proportion to the variations in gamma from roll to roll.

The actual effect of depletion along the developer flow for the flight images is much less than that implied by the sensitometric step wedge measurements for two reasons: (1) The flight exposures are chosen such that the density values in the region of interest are within the straight line portion of the D log E curve to

provide energy resolution. (2) The size of the solar image on the film is much smaller than the size of the sensitometric exposure (24 mm x 18 mm vs. 121 mm x 10 mm), thus requiring much less developer for equivalent exposures. Furthermore, the size of the most dense region in a solar image, the core of a solar active region, is of the order of 0.5 mm. Since the active region spatial scale is less than the spacing between successive layers of film in the development reel, one would expect the mixing of the solution on these scales to make local developer depletion negligible. This expectation is borne out in the analysis described in the fourth section of this paper, where a local variation of the shape of the D log E curve in the longer exposures would become apparent in comparison with the shorter exposures. No localized developer depletion effects have been found in any analysis of the flight images.

Even the worst case variations in the automated film processor performance are greatly superior to performance obtained by hand development of SO-212 film, where seemingly random localized variations in density are found of the order of 0.20 density units throughout most of the D log E curve. The new automated processor does not match the consistency of performance from roll to roll of film obtained with the Skylab effort, but since all the film from a flight is developed in one load, the roll to roll variations are not as important. The consistency of performance within a given development load of film is comparable between the new processor and the Skylab machine. With careful attention to the inclusion of calibration white light and the appropriate X-ray sensitometric step wedge exposures with the development of a roll of film, excellent photometric results are obtained with the new system.

3. PHOTOGRAPHIC MEDIA

In preparation for the S-054 X-Ray Spectrographic Telescope Skylab mission, a special order photographic film was procured from Eastman Kodak in 1973. This film, labeled SO-212, is a standard aerographic emulsion with panchromatic response and was obtained without a gelatin top coat to improve its soft X-ray sensitivity. This stock of SO-212 has been used as the primary detector of the AS&E X-ray Imaging Sounding Rocket Program since its manufacture. The large volume required for a minimum special order makes it impractical to consider the manufacture of another batch of SO-212 (or an improved special order film) for the sounding rocket program. However, the considerable stock (in sounding rocket terms) left over from the Skylab mission has been kept in refrigerated storage and, other than an increase in the base density level by 0.05 to 0.07 diffuse density units, retains the same level of X-ray performance to within the uncertainty of variations in film processing and X-ray sensitometry.

Two main drawbacks exist in the use of SO-212 in the X-ray imaging sounding rocket program. The first drawback is the difficulties in handling the film which are described above. The second drawback is the level of granularity of the emulsion and the ultimate spatial resolution of the film relative to the plate scale of the telescope. Visible light tests with fine grain film show that the X-ray rocket mirror possesses angular resolution slightly better than 1 arc second, while both visible light test and X-ray flight images on SO-212 demonstrate resolution of several arc seconds at best.[6]

Listed in Table 1 are the candidates we have considered as supplements to the SO-212 film in an attempt to improve spatial resolution and handling. The T-Max 100

film has been used in the sounding rocket flight of an XUV telescope by Hoover et al.[7], but we have not tested it. The SO-253 High Speed Holographic film was tested by AS&E during a flight on 31 January 1978.[8] The Technical Pan 2415 (TP2415) was tested by AS&E during a flight on 15 August 1987.

TABLE 1 - PHOTOGRAPHIC FILM COMPARISON
(Kodak Technical Data based on visible light performance)

Film Designation	RMS Granularity	Resolution (lines/mm)
* SO-253 High Speed Holographic	< 5	1250
* Technical Pan 2415	From < 5-8 depending on development	320
T-Max 100	8	160
SO-212 Special X-Ray Emulsion Manufactured for Skylab Mission	20	160

* Available only with gelatin top coat.

X-ray sensitometry was conducted for the films which were flown and the results are presented in Figure 1. The development parameters used in this comparison for all three films are those producing the desired speed and contrast for SO-212. It is possible to somewhat modify the characteristic curves of TP2415 and SO-253 through changes in development parameters to obtain a better suited response for a given application, but the baseline of X-ray performance in Figure 1 is useful for comparison purposes.

The X-ray sensitivity of photographic film is obviously inversely proportional to the grain size and resolution. It has not been practical at this point to obtain low energy (44 Angstrom) sensitometry of the ultra-high resolution SO-253 film because the response of this film requires a month-long exposure with our current apparatus. The effect of the top coat on the TP2415 appears to be minimal since there does not appear to be a great difference in the 8.3 Angstrom and 44 Angstrom performance relative to the SO-212 performance. Although a quantitative determination of the relative importance to soft X-ray photographic response of grain size and top coating must await parameterization of these results in terms of a model such as that of Henke et al.[9], it is useful to speculate on this subject. In a film with a fine grain structure, the higher volume fraction of AgBr grains implies a photon will, on average, traverse a smaller path length of emulsion gelatin before absorption by a developable grain relative to a more coarse grain film. It seems reasonable that the disadvantage of a top coat is compensated for by the reduction in gelatin traversed by a photon in the emulsion of TP2415 in comparison to SO-212. Higher maximum density in the shoulder region is expected in the more densely packed fine grain films. At lower energies, the decrease in penetration depth may minimize this effect.

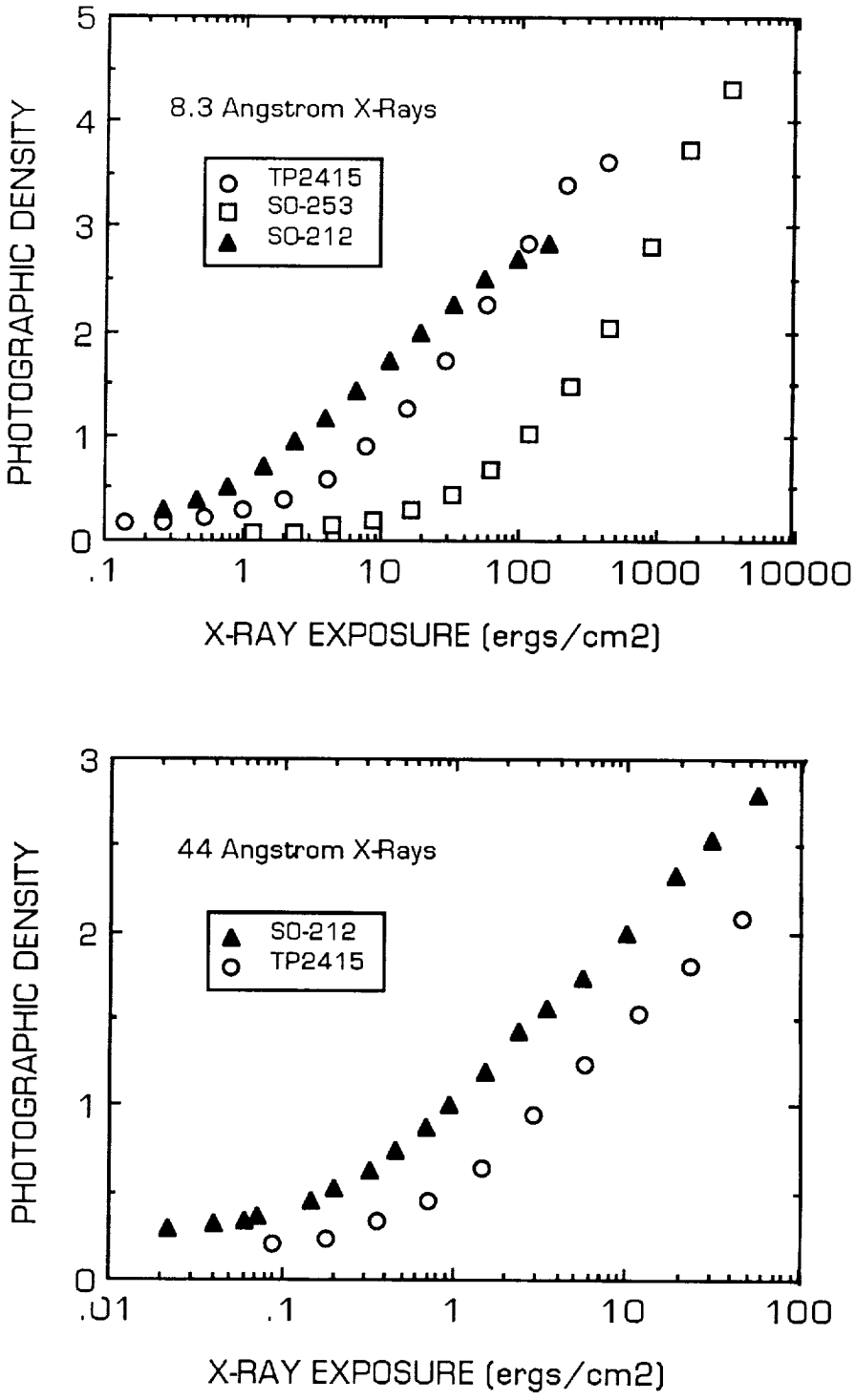

Figure 1. X-Ray Sensitometry of Photographic Film used in AS&E Solar Astronomy Soft X-Ray Imaging Sounding Rocket Program.

In practice, the target exposure times for SO-253 and TP2415 are increased relative to that of SO-212 by 5.5 and 2 stops, respectively. Since a typical sounding rocket flight provides about 5 minutes of observing time, the SO-253 is restricted to observations of bright active region cores and flares while the TP2415 can be used for everything but faint structures such as coronal holes and streamers. The SO-253 solar images show the active region cores resolved into loops in most regions with widths on the order of 1 arc second. The resolution of the TP2415 images fall midway between the resolution seen in the SO-253 images and that seen in the SO-212 images. The core regions which are resolved in the TP2415 images show complexes of loops with widths of 2 arc seconds.

An attempt is made to reproduce examples of these images in Figures 2 and 3. The limitations of photographic reproduction in these proceedings restricts the differences which can be shown. In Figure 2, a flaring bright point is clearly resolved into a loop like structure approximately 12 arc seconds long and 1 arc second wide in the SO-253 image of frame (c). The interpretation of this feature from the best SO-212 exposure in frame (b) would be that of a small linear region. It is impossible to identify any structure in the SO-212 image in frame (a) that was taken through the same filter as the SO-253 image of frame (c). In Figure 3, the differences between the TP2415 and the SO-212 are more subtle but still quite apparent in the original prints. The grain of the TP2415 is much finer than that of the SO-212, resulting in a higher confidence in the determination of the outline of these inherently diffuse structures. The arrow in frame (b) points to one of three small loops (approximately 2 arc-seconds wide and 8 arc-seconds long) in the southern boundary of Active Region 4839 that are resolved in the TP2415 images but not in the SO-212 images. The arrow in frame (d) points to the core loop system of the arcade of Active Region 4841 that is resolved into individual loops (approximately 2 arc-seconds wide and 1 arc-minute long) in the high temperature TP2415 image but is not resolved in the corresponding SO-212 image.

These results are very encouraging. Each of the three film types has a specific advantage that will be exploited in future flights. Because it is easy to compare the results from the very well calibrated SO-212 with the considerable archival X-ray coronal images, this film will remain the baseline film for the synoptic aspect of these investigations.

4. DETERMINATION OF THE FILM CHARACTERISTIC CURVE

Quantitative information about the properties of the coronal plasma can be obtained from soft X-ray solar images only if the film characteristic curve (i.e., the relationship between the photographic density of the image and the energy incident upon the film) is known. The determination of the applicable characteristic curve is significantly complicated by the fact that the film response is wavelength dependent and the wavelength distribution of the incident broadband spectrum through a given filter is not known a priori. Therefore, the determination of the film characteristics curve must be an iterative process. The wavelength dependance of the X-ray response of the SO-212 was determined through an exhaustive effort conducted during the S-054 Skylab Program[3,4]. The measured wavelength response of the film is combined (through a weighted average) with a model of the X-ray emission of a plasma with assumed temperature, density, ionization state, and composition (folded with the transmission function of the telescope and filter) to produce a modeled characteristic curve. This modeled curve must be compared with the photographic data from the flight in a convenient way, as the plasma parameters

Figure 2. Flaring Bright Point photographed on January 31, 1978.

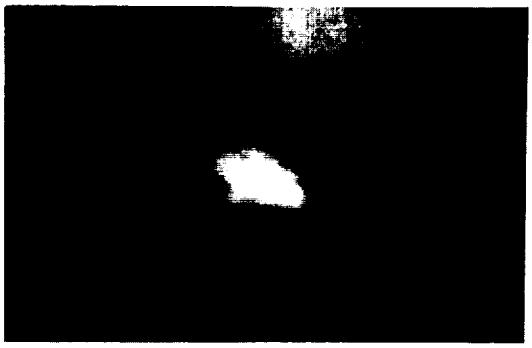

(a)

WAVEBAND 8-39, 44-64Å
FILM S0-212
EXPOSURE 0.9 sec.

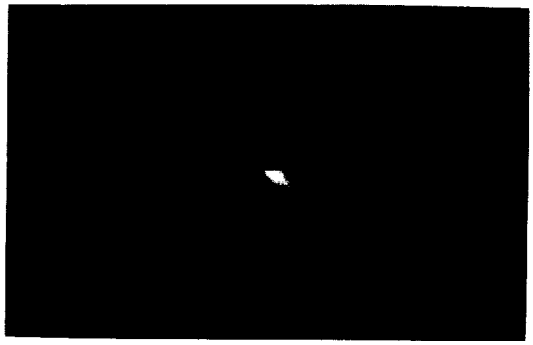

(b)

WAVEBAND 8-20Å
FILM S0-212
EXPOSURE 0.7 sec.

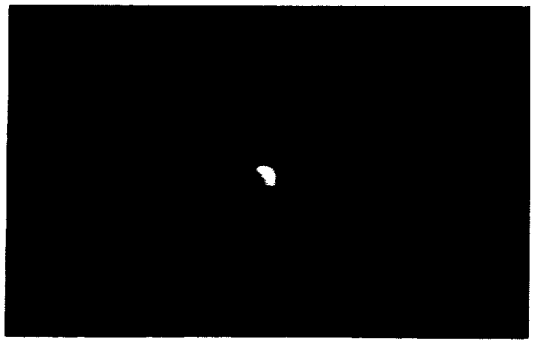

(c)

WAVEBAND 8-39, 44-64Å
FILM S0-253
EXPOSURE 20.3 sec.

1 arc min.

Figure 3. Active Region complexes 4842, 4841, and 4839 in the southern hemisphere on August 15, 1987.

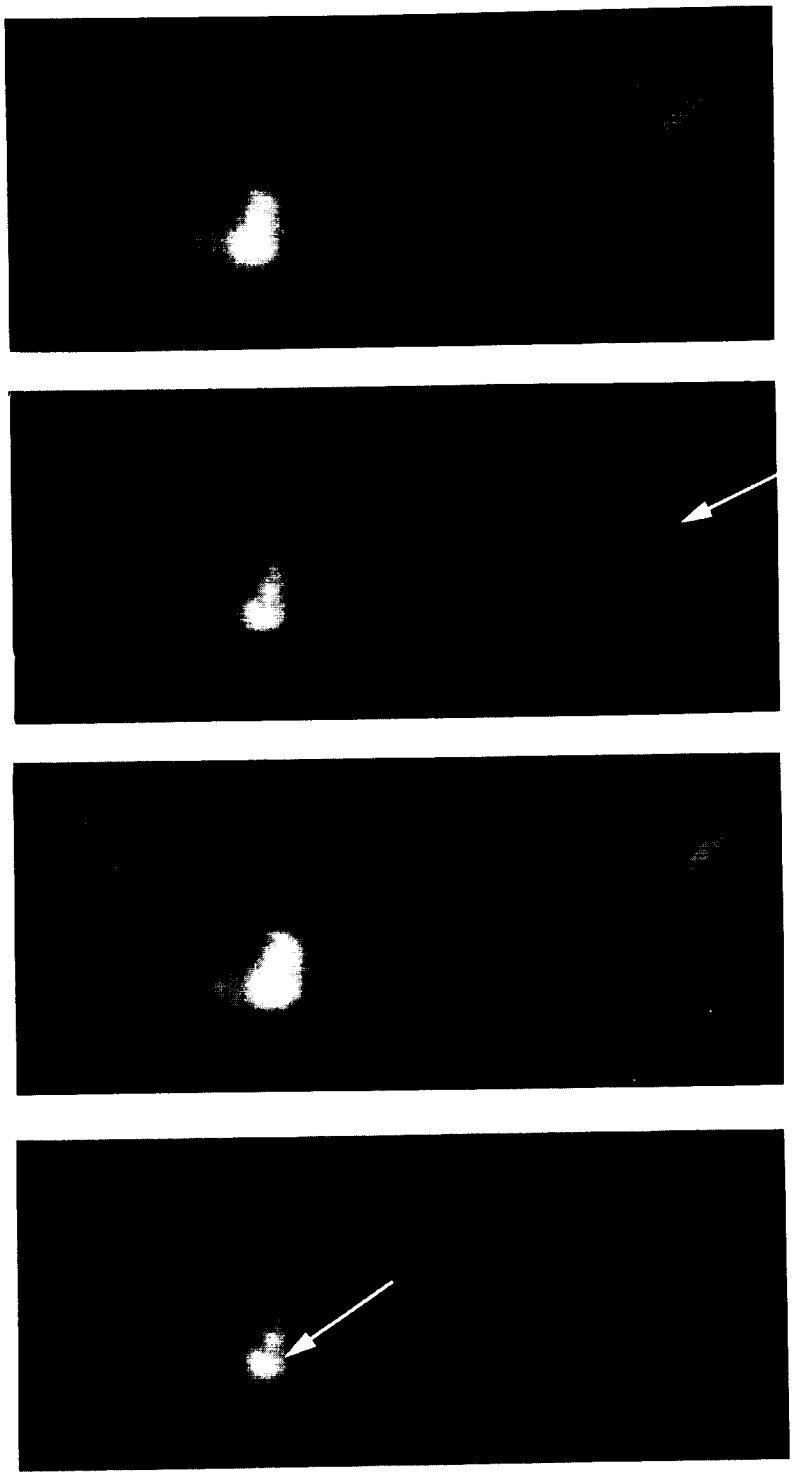

(a)

WAVEBAND 8-39, 44-60Å
FILM S0-212
EXPOSURE 3 sec.

(b)

WAVEBAND 8-39, 44-60Å
FILM TP2415
EXPOSURE 9 sec.

(c)

WAVEBAND 8-20Å
FILM S0-212
EXPOSURE 9 sec.

(d)

WAVEBAND 8-20Å
FILM TP2415
EXPOSURE 20 sec.

5 arc min.

are iteratively adjusted to obtain a good fit to all the plasma diagnostics of these measurements.

For this discussion, we will use a parameterization of the film characteristic curve that was developed by VanSpeybroeck for the Skylab S-054 data analysis; it has been found to fit experimental film characteristic curves well. Other functional forms have been used to describe D log E curves (Tsubaki and Engvold[10], Cook et al.[1]); the VanSpeybroeck form is chosen for this analysis, as its parameters relate to quantities which can be easily measured from an experimental film characteristic curve. The VanSpeybroeck form of the relationship between the photographic density on the film is:

$$D = D_{base} + D_{max} + k \int_{a\mu E}^{\infty} \frac{e^{-z}}{z}\, dz - k \int_{a\mu E e^{-D_{max}/k}}^{\infty} \frac{e^{-z}}{z}\, dz$$

where:
- D = net density on the film
- E = power per unit area deposited on the film
- D_{base} = density of the base fog level
- D_{max} = maximum possible net density
- au = film speed parameter, proportional to the reciprocal of the energy at which the density equals D_{base} in the extrapolation of the linear portion of the curve.
- k = the slope of the linear portion of the ln E vs. D curve

The relationship between k (the slope of the characteristic curve expressed in terms of the natural logarithm of energy) and gamma (the slope of the characteristic curve expressed in the traditional terms of the logarithm base-ten of energy) is

$$\text{gamma} = 2.3\ k$$

The four parameters of the characteristic curve to be determined are D_{base}, D_{max}, au, and gamma. D_{base} and D_{max} do not vary with wavelength, so these values can be measured in the laboratory. The other two parameters, au and gamma, are wavelength dependent and must be determined by an iterative technique.

Two methods of comparing a trial parameterized characteristic curve to the flight data have been utilized:

1. The scatter plot technique, which was developed as part of the Skylab ATM experiment data analysis of broadband soft X-ray images of the solar corona.

2. The density histogram technique, which was developed by Cook, Ewing, and Sutton[1] for the analysis of UV photographic spectra of the Sun.

By both of these techniques, the energy calibration is an iterative process between the laboratory calibration of the film and the flight data: The D-to-E calibration curve measured in the lab from a stepwedge, generated with monochromatic X-rays of a wavelength approximating the mean of the bandpass of the relevant filter, is used as a first approximation to the film characteristic curve. This approximation is refined iteratively by comparing image with different exposure times. The scatter plot and density histogram techniques differ in the methods used for image comparison.

The Scatter Plot Technique

By this technique, two digitalized images of differing exposure are, pixel by pixel, transformed and compared to determine the energy calibration curve. The images used must be co-aligned images of the same region, taken close enough together in time that the region can be assumed not to have changed between exposures. The trial D log E curve, taken from the monochromatic stepwedge, is used to convert the photographic densities $(D_1)_i$ and $(D_2)_i$, of each pixel, i, from each of the two exposures to powers per unit area, $(E_1)_i$ and $(E_2)_i$. A "scatter plot" is constructed by plotting E_1 vs. $(t_2/t_1)\ E_2$, where (t_2/t_1) is the ratio of the exposure times. If the slope of the best fit straight line to the scatter plot is unity, the film characteristic curve is correct. If not, au and gamma are varied. The procedure is then repeated until no improvement in the scatter plot can be made. Note that the accuracy of this method is critically dependent upon the distribution of the points within the scatter plot. Furthermore, the scatter plot provides little sensitivity to, and feedback for, the toe region of the characteristic curve.

The Density Histogram Technique

This technique is the application of a method described by Cook et al.[1] for determining the film characteristic curve by transforming and comparing density histograms from images of differing exposures. Histograms of density are constructed from at least two digitalized images of the same region of the Sun, taken with different exposure times. One of the exposures is chosen as the base exposure, and bin-by-bin the histograms for the other exposure times are constructed from the base using the trial D log E curve, obtained from a monochromatic stepwedge. These transformed histograms are compared to the actual histograms of the appropriate exposure. The parameters of the characteristic curve, au and gamma, are varied iteratively until the best match is found between the transformed histograms and the actual histograms.

This technique was used to determine the characteristic curves for film from the 11 December 1987 AS&E sounding rocket flight. The monochromatic reference stepwedge for this film is shown in Figure 4. Also plotted in Figure 4, is the fit to the stepwedge data obtained with the density histogram technique, for which $D_{base} = 0.16$, $D_{max} = 3.35$, au = 5.70, and gamma = 0.89. It is apparent in Figure 4 that the density histogram technique provides the means to determine an excellent fit to the data of the characteristic curve parameters. Presented in Figure 5 is the characteristic curve determined by the density histogram technique using 3 s, 9 s, and 30 s exposures through the 8-39, 44-64 Angstrom bandpass filter of Active Region 4901, obtained during the 11 December 1987 flight of the AS&E Solar Rocket Payload. Also plotted for comparison in Figure 5 are the values of the monochromatic reference stepwedge shown in Figure 4. The final values of the parameters of the flight data characteristic curve were: $D_{base} = 0.16$, $D_{max} = 3.35$, au = 7.00, and gamma = 0.91.

Although a determination of the characteristic curve by the scatter plot technique has not yet been completed for the image of Active Region 4901, in the data analysis of previous flights of this payload, the values of au and gamma determined by the scatter plot technique for the comparable flight data are on the order of 10 to 20 percent greater than those determined for the reference 44 Angstrom

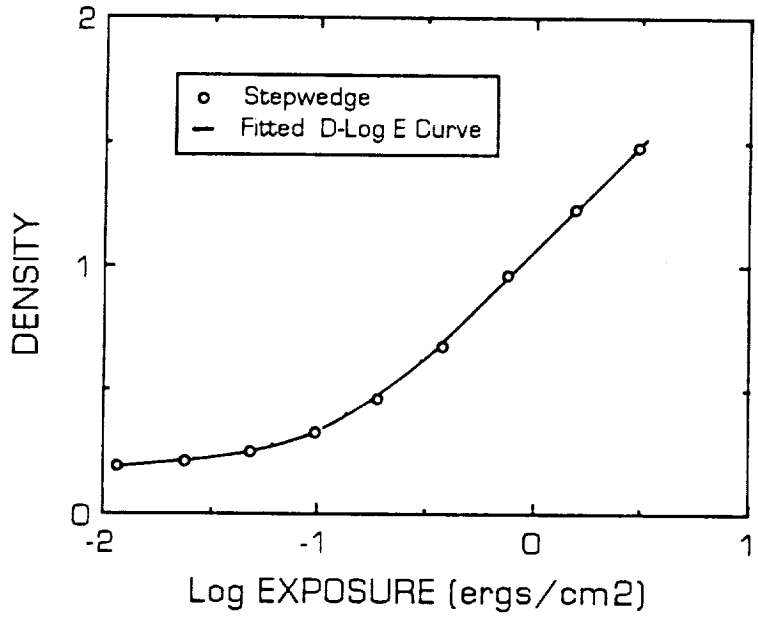

Figure 4. The 44 Angstrom monochromatic reference stepwedge for the 11 December 1987 rocket flight and the D log E curve fitted to this stepwedge data using the density histogram technique. (D_{base} = 0.16, au = 5.70, and gamma = 0.89).

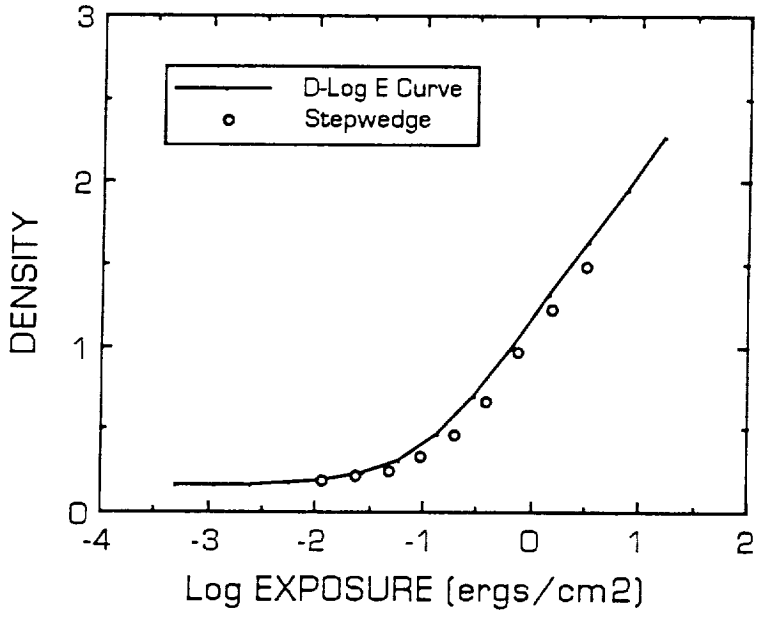

Figure 5. The characteristic curve for images from the 11 December 1987 rocket flight, as determined by the density histogram technique using 3 s, 9 s, and 30 s exposures through a polypropylene filter. (D_{base} = 0.16, au = 7.00, and gamma = 0.91). The reference 44 Angstrom monochromatic stepwedge steps previously shown in Figure 4 are plotted again for comparison.

monochromatic stepwedge. Thus, both techniques find the same qualitative difference between the actual flight data and the reference monochromatic stepwedge data. As can be seen in Figure 5, making the assumption that the reference monochromatic stepwedge characteristic curve is equivalent to the flight data characteristic curve leads to an over-estimate of energy deposit in the focal plane by as much as 50 percent. The importance of this aspect of the image analysis is clear.

Discussion

The density histogram technique is expected to be the more reliable method of energy calibration for the following reasons:

1. The accuracy of the image co-alignment is less critical in the statistical approach of the density histogram technique. The pixel-by-pixel comparison of the scatter plot technique requires more exact co-alignment of the images.

2. As many exposures as are available may be used simultaneously to determine the characteristic curve by the density histogram technique. The scatter plot technique can compare two exposures only.

3. The density histogram technique is much less sensitive to the distribution of density values within a given exposure, and works well in the toe region of the characteristic curve.

4. It is easier to identify and ignore dirt, scratches, background, etc in the density histograms than in scatter plots.

We are only in the initial stages of implementing the density histogram technique in the analysis of flight data. A parallel effort with the scatter plot technique is planned for comparison. The initial results of the density histogram technique are very encouraging.

5. CONCLUSION

Three improvements in photographic X-ray imaging techniques for solar astronomy have been presented. The testing and calibration of a new film processor has been conducted, and the resulting product will allow photometric development of sounding rocket flight film immediately upon recovery at the missile range. Two fine-grained photographic films have been calibrated and flight tested to provide alternative detector choices when the need for high resolution is greater than the need for high sensitivity. An analysis technique used to obtain the characteristic curve directly from photographs of UV solar spectra has been applied to the analysis of soft X-ray photographic images, and the resulting procedure provides a more complete and straightforward determination of the parameters describing the X-ray characteristic curve than previous techniques. These improvements fall into the category of refinements instead of revolutions, indicating the fundamental suitability of the photographic process for X-ray imaging in solar astronomy. Although development of electronic detectors is the central component of our on-going development effort, photographic media will continue to be our baseline director for the near future.

6. ACKNOWLEDGEMENTS

We would like to acknowledge the crucial assistance and guidance of Robert Haggerty during all aspects of photometric film development in the AS&E Solar Physics Program. Anna Franco and Daniel O'Mara provided significant laboratory support to this project. We would like to thank S. Kahler, A. Krieger and D. Webb for useful discussions. This work builds on the strong tradition of quantitative image analysis that is a hallmark of AS&E. This work was supported by NASA contract NAS5-25496 and NASA GSRP Grant NGT-50308.

7. REFERENCES

1. Cook, J.W., Ewing, J.A., and Sutton, C.S., Pub. Astro. Soc. of the Pacific 100, 402, 1988.

2. Vaiana, G.S. VanSpeybroeck, L., Zombeck, M., Krieger, A.S., Silk, J.K., and Timothy, A.F., Space Sci. Inst. 3, 19, 1977.

3. Haggerty, R., Simon, R., Golub, L., Silk, J.K., Timothy, A.F., Krieger, A.S., and Vaiana, G.S., AAS Photo. Bull. 10, 8, 1975.

4. Simon, R., Haggerty, R., Golub, L., Krieger, A.S., Silk, J.K., and Timothy, A.F., Presented at the AAS Working Group on Photographic Materials, Rochester, NY, August 1974.

5. Krieger, A.S., SPIE, 106, 24, 1977.

6. Davis, J.M., Krieger, A.S., Silk, J.K., and Chase R.C., SPIE 184, 96, 1979.

7. Hoover, R.B., Barbee, T.W., Lindblom, J.F., and Walker, A.B.C., Kodak Tech Bits, pp. 1-6, June 1988.

8. Davis, J.M., Quarterly Progress Report No. 11, Contract NAS2-8683, 1977.

9. Henke, B.L., Kwok, S.L., Uejio, J.Y., Yamada, H.T., and Young, G.C., J. Opt. Soc. Am. B 1, 818, 1984.

10. Tsubaki, T. and Engvold, O., AAS Photo-Bulletin 9, 17, 1975.

4.23 Correspondence Between Solar Fine-Scale Structures in the Corona, Transition Region, and Lower Atmosphere from Collaborative Observations

D. Moses

American Science and Engineering, Inc.
Cambridge, Massachusetts 02139

J.W. Cook, J.-D.F. Bartoe, G.E. Brueckner, K.P. Dere

Naval Research Laboratory
Washington, D.C. 20375-5000

D. Webb

Emmanuel College
Boston, Massachusetts

J.M. Davis

NASA/Marshall Space Flight Center
Huntsville, Alabama

F. Recely

National Solar Observatory
Tucson, Arizona

and

S.F. Martin and H. Zirin

Big Bear Solar Observatory
Pasadena, California